2011 American Control Conference
on O'Farrell Street, San Francisco, CA, USA
June 29 - July 01, 2011

Efficient Minimum Manoeuvre Time Optimisation of an Oversteering Vehicle at Constant Forward Speed

Julian P. Timings and David J. Cole*

Abstract— **A receding horizon steering controller is presented, capable of pushing an oversteering nonlinear vehicle model to its handling limit while travelling at constant forward speed. The controller is able to optimise the vehicle path, using a computationally efficient and robust technique, so that the vehicle progression along a track is maximised as a function of time. The resultant method forms part of the solution to the motor racing objective of minimising lap time.**

I. INTRODUCTION

The research presented here focuses on the development of a virtual racing driver model capable of minimising the manoeuvre time of a vehicle over a predefined course. Such work is motivated by the desire to achieve a greater understanding of the interaction between a driver and vehicle operating at its limit of capabilities. A greater appreciation for how a driver arrives at a particular decision, might in turn allow a race car to be developed more closely tailored to a driver's needs.

A racing driver is required to find the balance of vehicle controls that results in the fastest possible lap time. This is achieved by maximising the velocity of the vehicle throughout the manoeuvre, limited periodically by the available tyre grip and power output of the vehicle's engine. Simultaneously the driver attempts to choose a vehicle trajectory that minimises the total distance travelled. These two requirements are conflicting in nature and hence a compromise is sought which results in vehicle manoeuvre time being minimised.

A number of attempts have been previously made by researchers to solve the minimum lap time problem. An approach widely adopted by racing establishments is the so called quasi-steady-state (QSS) method [1], [2]. This approach approximates the motion of the car as a series of steady state manoeuvres which can be joined together to form a complete vehicle-circuit simulation. However, the steady-state assumption means that vehicle transient behaviour cannot be studied. Furthermore, the approach has no consideration of the human driver, meaning it has limited use during the vehicle design phase.

More recently, to permit the study of vehicle transients a number of new methods, based on optimal control theory, have been developed. Thommyppillai *et al.* [3], [4] have developed an approach centered around optimum path following. The concept relies on the idea that accurately tracking a predefined racing line while trying to maximise vehicle speed results in an optimum lap. The approach, however, is somewhat restrictive in nature as the racing line is fixed regardless of the vehicle setup parameters, similar to the QSS lap simulation methods. A second stream of research has proposed the problem as one of nonconvex nonlinear optimisation with constraints used to reflect the track boundaries and prohibited vehicle operating regions. This method enables both the optimum path and speed trajectories to be computed online with full account of vehicle nonlinearities. Such methods have successfully been developed by a number of researchers [5], [6], [7]. However, solving the required nonconvex optimisation problem is extremely computationally intensive and the techniques generally have a lack of robustness.

In [8], the initial results of a computationally efficient method for optimising the vehicle path around a racing track of finite width were presented. The work presented here extends this earlier research by providing a refined algorithm, directly extendable to the case of combined path and speed optimisation. It focuses particularly on the improved methods used to linearise the problem and thus ensure the optimisation problem remains convex and therefore computationally efficient. Simulations demonstrating the control of an oversteering vehicle are also presented.

The next section gives an overview of the oversteering nonlinear vehicle model used for both the vehicle plant and internal human model. This is followed by descriptions of the various components that make up the steering controller. The method used to generate the optimum vehicle trajectory is next outlined together with the how the vehicle position relative to the track is linearised which ultimately results in an efficient computational problem. Finally, a number of simulation results are presented.

II. VEHICLE MODEL

The lateral dynamics of the vehicle are represented using the standard single track yaw/sideslip model shown in Fig. 1. The equations of motion for lateral velocity, v, and yaw rate, $\dot{\psi}$, can therefore be written as:

$$M_t(\dot{v} + u\dot{\psi}) = F_{yf} + F_{yr} \tag{1}$$

$$I_{zz}\ddot{\psi} = aF_{yf} - bF_{yr} \tag{2}$$

which are valid for the constant longitudinal velocity case provided small angles are assumed. The pure lateral slip force characteristics of the tyres are assumed to vary according to the *Magic Formula* expression:

J. P. Timings and D. J. Cole are with the Department of Engineering, Driver-Vehicle Dynamics Group, University of Cambridge, Trumpington Street, Cambridge, CB2 1PZ, UK

* Corresponding author: david.cole@eng.cam.ac.uk

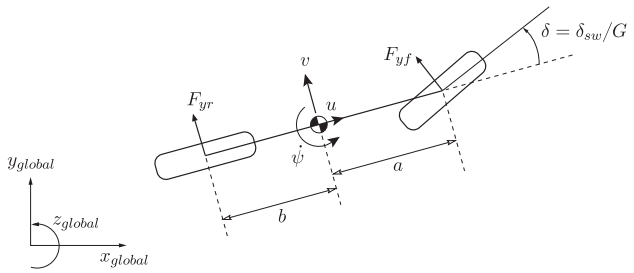

Fig. 1. Single track vehicle model with associated forces and dimensions.

$$F_{yj} = -2D_j \sin\left(C_{yj} \arctan(B_{yj}\alpha_j - E_{yj}(B_{yj}\alpha_j - \arctan(B_{yj}\alpha_j)))\right) \tag{3}$$

The tyre nonlinearities are approximated using a Linear Time Varying (LTV) model. Front and rear lateral slips, α_f and α_r are chosen as set point parameters about which the tyre characteristics are linearised. Collecting only first order terms of a Taylor Series expansion enables the front and rear lateral force of the tyres to be described by the simple LTV expression:

$$F_{yj(t)} = C_{jy(t)}\alpha_{j(t)} + D_{jy(t)}, \tag{4}$$

where $C_{jy(t)}$ and $D_{jy(t)}$ denote the time varying lateral slip stiffness and tyre force intercept at zero slip respectively [9].

Furthermore, the vehicle system to be controlled is considered to comprise of the vehicle dynamics coupled with the driver's Neuromuscular System (NMS) dynamics. As demonstrated in [10], the NMS can be represented as an under-damped second order system which acts on the steering input to the vehicle, thus

$$\ddot{\delta}_{sw} + 2\zeta_n\omega_n\dot{\delta}_{sw} + \omega_n^2\delta_{sw} = \omega_n^2\delta_{com}, \tag{5}$$

where δ_{com} is the steering wheel angle commanded from the driver's brain and δ_{sw} considered an output of the driver's NMS. ζ_n and ω_n denote the damping ratio and natural frequency of the NMS respectively.

Combining the NMS model and vehicle dynamics allows the total system to be represented using a discrete time state-space description:

$$x_{(k+1)} = A_{(k)}x_{(k)} + B_{(k)}\Delta\delta_{com(k)} + E_{(k)} \tag{6}$$

$$z_{(k)} = C_{(k)}x_{(k)}, \tag{7}$$

where $x_{(k)}$ is the vehicle system states, $E_{(k)}$ contains the tyre force intercept terms from (4) and the commanded steering input has been split into the sum of the steering input from the previous time step, now a system state, and the change in steering input during the present step.

The chassis, tyre and NMS parameters used to construct the vehicle system are given in Table I. Note that the distances from the front and rear axles to the vehicle CoG result in a vehicle with a rear bias weight distribution.

TABLE I
VEHICLE, TYRES AND DRIVER'S NMS PARAMETERS.

Parameter	Symbol	Value
Vehicle mass	M_t	1050 kg
Vehicle yaw inertia	I_{zz}	1500 kgm^2
CoG to front axle distance	a	1.38 m
CoG to rear axle distance	b	0.92 m
Steer to road wheel angle ratio	G	17
Stiffness factor (per tyre)	B_{yi}	17.5
Shape factor (per tyre)	C_{yi}	1.68
Peak factor (per tyre)	D_{yi}	3900 N
Curvature factor (per tyre)	E_{yi}	0.6
NMS damping ratio	ζ_n	0.7
NMS natural frequency	ω_n	18.9 rads^{-1}

III. STEERING CONTROLLER

The steering controller is structured to form a nonlinear Model Predictive Control (MPC) strategy. However, in order to reduce the computational demand, the controller does not generate a fully optimal nonlinear control law, but instead makes use of time varying internal models, linear (in)equality constraints and a quadratic cost to form a convex Quadratic Programming (QP) problem. Formulating the optimisation problem in this way guarantees its termination and allows it to be solved rapidly using a number of possible methods [11].

A. Preview and Predicted Vehicle Trajectory

Central to the controller's ability to minimise manoeuvre time is the idea of a preview window ahead of the vehicle gathering information and using this as the basis for control decisions. Employing such a strategy aims to mimic the line of sight of a real driver and their ability to assess the track ahead and make steering (and brake/throttle) decisions accordingly. The internal model produces a future predicted response of the vehicle at each iteration. Here, the internal model is taken to be the LTV vehicle model developed in section II. The previous prediction results (at time step $k-1$) can therefore be used to gather the necessary preview information for the next optimsation. In what follows the track centreline is taken as the reference trajectory on which preview information is based. Fig. 2 sets out the reference trajectory parameters and how they relate to the predicted vehicle trajectory.

As shown in Fig. 2, the track centreline is defined in the global reference frame using an intrinsic coordinate description (s_r, ϕ_r). The previous predicted position of the vehicle is defined relative to lines normal to the track centreline and at lateral displacements errors $y_{err(k+i|k-1)}$ for $i = 1 \ldots N_p$ where N_p is the prediction horizon.

In order to determine the future vehicle position, the *variable-model-preview* concept detailed by Keen and Cole [9] is adopted. This approach allows for a more accurate estimation of the vehicle's future state and output trajectories, $\hat{x}_{(k+i)}$ and $\hat{z}_{(k+i)}$ respectively, by using the discarded input commands from the previous control cycle. Iterating (6), open-loop, with the series of delta input commands, $\Delta\hat{\delta}_{com(k+i-1)}$ for $i = 1 \ldots N_p$, enables an estimation of the predicted trajectory for the next control cycle to be found. Since (6) and (7) are time varying in nature the

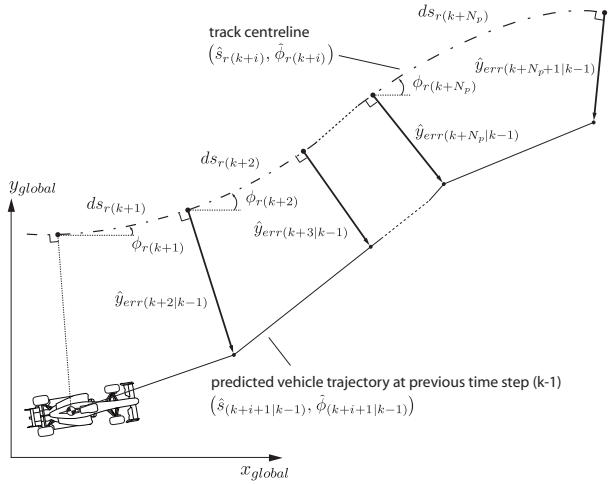

Fig. 2. Predicted vehicle trajectory and corresponding reference trajectory parameters.

prediction results in a sequence of linearised vehicle models that approximate the future dynamics of the vehicle along the horizon. This future knowledge of the expected vehicle dynamics enhances the prediction strategy and is an essential part of the control strategy.

B. Banded MPC Scheme

The following quadratic cost function is proposed to connect the linearised vehicle dynamics within the predicted trajectory and the reference trajectory.

$$\begin{aligned} J_{(k)} &= \sum_{i=1}^{N_p} \hat{z}^T_{(k+i)} Q_{1(i)} \hat{z}_{(k+i)} + R_{(i)} \Delta\hat{\delta}^2_{com(k+i-1)} \\ &+ Q^T_{2(i)} \hat{z}_{(k+i)}, \end{aligned} \tag{8}$$

where $Q_{1(i)}$ and $Q_{2(i)}$, are semi-positive definite diagonal matrices which contain the weights of relative importance placed on the output objectives. The positive scalar, $R_{(i)}$ determines the extent to which the change in steering demand, $\Delta\hat{\delta}_{com}$, contributes to the minimisation of the cost function. Typically when forming MPC problems the predicted states $\hat{x}_{(k+i)}$ are eliminated from the problem, instead written as functions of the current state and optimised control inputs. However, as demonstrated in [12], by not eliminating the predicted states the resultant QP problem has a banded structure in which the sparsity can be exploited by suitably developed solvers. The technique is particulary advantageous when using long preview/control horizons and results in rapid convergence to solution when compared to the equivalent densely structured QP problem. To implement the banded structure the following *equality* constraint is therefore introduced:

$$\hat{x}_{(k+i+1)} = \hat{A}_{(k+i)} \hat{x}_{(k+i)} + \hat{B}_{(k+i)} \Delta\hat{\delta}_{com(k+i)} + \hat{E}_{(k+i)}, \tag{9}$$

for $i = 0 \ldots N_p - 1$.

By substituting the linearised state-space output equation (7) into the quadratic cost (8) and writing in a more compact form, the general QP problem with equality constraint (9) and the possibility of *inequality* constraints on the predicted input and output trajectories can be written as

$$\min_{\theta_{(k)}} J_{(k)} = \frac{1}{2} \theta^T_{(k)} H_{(k)} \theta_{(k)} + \eta^T_{(k)} \theta_{(k)} \qquad (H_{(k)} = H^T_{(k)} \geq 0) \tag{10}$$

subject to

$$\Gamma_{(k)} \theta_{(k)} = \gamma_{(k)} \tag{11}$$

and

$$\Omega_{(k)} \theta_{(k)} \leq \omega_{(k)}, \tag{12}$$

where the resultant optimised variable has the following structure

$$\theta_{(k)} = \begin{bmatrix} \Delta\hat{\delta}_{com(k)} \\ \hat{x}_{(k+1)} \\ \Delta\hat{\delta}_{com(k+1)} \\ \hat{x}_{(k+2)} \\ \vdots \\ \Delta\hat{\delta}_{com(k+N_p-1)} \\ \hat{x}_{(k+N_p)} \end{bmatrix} \tag{13}$$

C. Optimum Path Generation

The objective of the controller is to minimise the time taken to perform a particular manoeuvre. Since in the present case the forward speed of the vehicle is considered constant, this can be achieved by determining a path that minimises the total distance travelled. With time as the independent variable, this is posed as maximising the distance travelled in a fixed amount of time [7]. From Fig. 3, the task is to describe the incremental distance ds_r, travelled along the track centreline, in terms of the incremental distance $ds = VT \approx uT$ travelled by the vehicle in time T. Maximising ds_r therefore maximises the progression of the vehicle along the track. All vehicle progression evaluations are made with respect to lines normal to the track centreline.

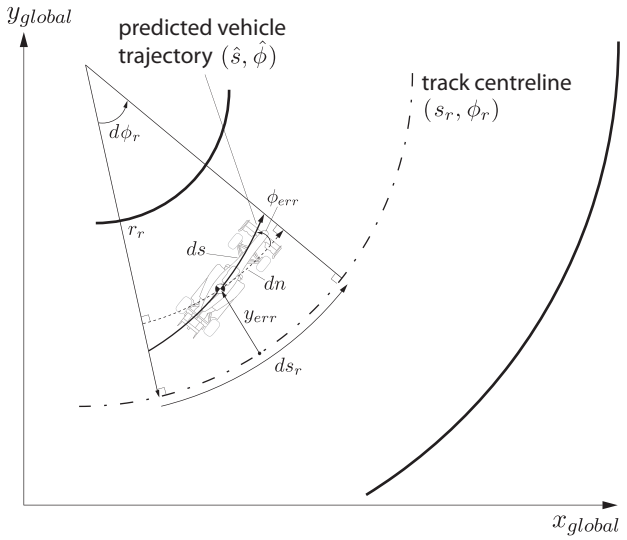

Fig. 3. Geometric definitions for derivation of intrinsic vehicle-track progression expression.

Fig. 3 allows the derivation of the following expression describing the incremental distance, ds_r, travelled along the track centreline in terms of heading angle and lateral displacement error between the predicted vehicle and track centreline:

$$ds_r = ds + y_{err} d\phi_r - ds\frac{\phi_{err}^2}{2}, \tag{14}$$

provided ϕ_{err} remains in the limit in which a second-order small angle approximation of cosine remains valid. Examining (14) reveals the connection between the various vehicle related terms and progression along the track. The first term, ds the distance the vehicle travels in one time step, connects directly the velocity of the vehicle to track progression. The term associated with the lateral error y_{err}, is positive when on the inside of the bend as drawn in Fig. 3. Hence progression along the track centreline is increased the further the vehicle moves to the inside of the bend. The term associated with ϕ_{err}, is negative since any angle error between the track and vehicle heading requires the vehicle to travel slightly further to achieve the same track progression compared to if it travelled in a direction parallel to the track centreline.

Summating expression (14) from $i = 1 \dots N_p$ yields the nominal distance travelled along the track centreline over the prediction horizon.

$$\sum_{i=1}^{N_p} ds_{r(k+i)} = \sum_{i=1}^{N_p} ds + \hat{y}_{err(k+i)} d\phi_{r(k+i)} - ds\frac{\hat{\phi}_{err(k+i)}^2}{2} \tag{15}$$

Therefore by maximising (15) the progress of the vehicle along the track in a fixed time interval $(N_p T)$ is maximised. Here, the longitudinal velocity is assumed constant and thus the summation of the first term can be neglected. It should be noted that in the event of optimising both the vehicle path and speed profile, as real racing drivers do, using (15) in its entirety for the objective function would permit this. For the constant speed case however, the following candidate objective function is proposed, taking into account possible penalisation of steering effort

$$\begin{aligned} J_{(k)} &= \sum_{i=1}^{N_p} q\Big(- \hat{y}_{err(k+i)} d\phi_{r(k+i)} + \frac{\hat{\phi}_{err(k+i)}^2}{2}\Big) \\ &+ R\Delta\hat{\delta}_{com(k+i-1)}^2, \end{aligned} \tag{16}$$

where q and R are the weights placed on maximising the distance travelled and the amount of the control effort used respectively. Equations (14)-(16) differ from their counterparts in [8], by providing a more accurate description of the progress of the vehicle relative to the track. Additionally, the objective function is no longer formed explicitly as a tracking/regulatory task.

In order for the optimisation to remain a convex QP problem, which can be solved in an efficient way, it is necessary that all the terms in (16) can be linearly reproduced from the system states and inputs. $\Delta\delta_{com}$ is the input to the system and hence can be produced straightforwardly. The track radius is approximated using $r_{r(k+i)} \approx r_{r(k+i+1|k-1)}$ from the previous predicted trajectory, likewise the heading angle error between the vehicle and track, $\hat{\phi}_{err}$, can be defined simply as

$$\begin{aligned} \hat{\phi}_{err(k+i)} &= (\hat{\beta}_{(k+i)} + \hat{\psi}_{(k+i)}) - \phi_{r(k+i)} \\ &\approx (\hat{\beta}_{(k+i)} + \hat{\psi}_{(k+i)}) - \phi_{r(k+i+1|k-1)}, \end{aligned} \tag{17}$$

for $i = 1 \dots N_p$, where the vehicle slip angle is approximated as $\beta \approx \frac{v}{u}$. However, the normal distance between the vehicle and track centreline, $\hat{y}_{err}$, is a nonlinear function in the system states. The next section details how $\hat{y}_{err}$ is linearised and therefore the linear positioning of the vehicle relative to the track preserved.

D. Linearising Lateral Displacement Errors

It is proposed that, provided there are only small changes between consecutive predicted trajectories, the lateral displacement error to be optimised at the current time step can be approximated using

$$\hat{y}_{err(k+i)} = \hat{y}_{err(k+i+1|k-1)} + \Delta\hat{y}_{err(k+i)} \tag{18}$$

It is therefore only necessary to derive a linear expression which describes the change in lateral displacement error between two successive predicted vehicle paths, $\Delta\hat{y}_{err(k+i)}$, rather than the absolute lateral error. With the vehicle forward speed considered constant, this depends only on the differences in heading angles between the two trajectories $\delta\phi$. Fig. 4 illustrates the connection between the two paths when an intrinsic coordinate description is used. Hence an approximation of the change in lateral displacements can be found using

$$\begin{aligned} \hat{\delta}_{y(k+i)}^{\delta\phi} &= \hat{\delta}_{y(k+i-1)}^{\delta\phi} \cos\left(\hat{\phi}_{(k+i+1|k-1)} - \hat{\phi}_{(k+i|k-1)}\right) \\ &+ ds(\hat{\phi}_{(k+i)} - \hat{\phi}_{(k+i+1|k-1)}) \end{aligned} \tag{19}$$

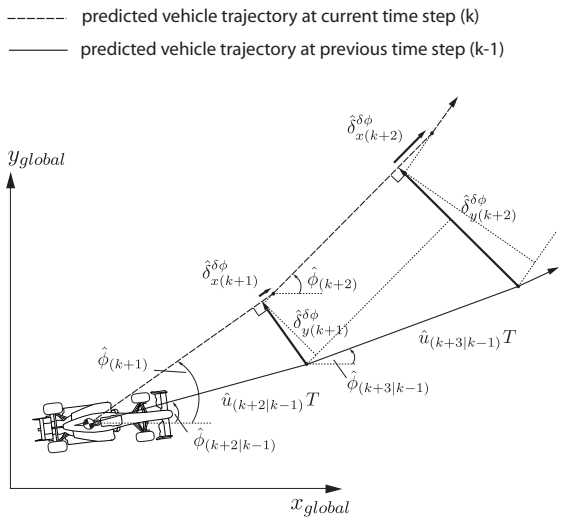

Fig. 4. Initial geometric definitions for derivation of intrinsic displacement error expressions, due to a change in heading angle $\delta\phi$, for two consecutive predicted vehicle paths.

where $\hat{u}_{(k+i)}T = \hat{u}_{(k+i+1|k-1)}T = ds$ for $i = 1 \dots N_p$. There is also a correspondingly small change in longitudinal displacement when the heading angle of the vehicle changes which ultimately contributes to $\Delta\hat{y}_{err}$. From Fig. 4 it is possible to approximate this as

$$\begin{aligned} \hat{\delta}^{\delta\phi}_{x(k+i)} &= \hat{\delta}^{\delta\phi}_{x(k+i-1)} \cos\left(\hat{\phi}_{(k+i+1|k-1)} - \hat{\phi}_{(k+i|k-1)}\right) \\ &+ \hat{\delta}^{\delta\phi}_{y(k+i-1)} \sin\left(\hat{\phi}_{(k+i+1|k-1)} - \hat{\phi}_{(k+i|k-1)}\right) \end{aligned} \quad (20)$$

By resolving the changes in lateral and longitudinal displacement, (19) and (20) respectively, in the direction normal to the track centreline, $\Delta\hat{y}_{err}$ can be approximated as

$$\begin{aligned} \Delta\hat{y}_{err(k+i)} &\approx \hat{\delta}^{\delta\phi}_{y(k+i)} \cos(\hat{\phi}_{err(k+i+1|k-1)}) \\ &+ \hat{\delta}^{\delta\phi}_{x(k+i)} \sin(\hat{\phi}_{err(k+i+1|k-1)}), \end{aligned} \quad (21)$$

for $i = 1 \dots N_p$, which results in a further improvement in accuracy compared to the equivalent quantity defined in [8]. By including $\hat{\delta}^{\delta\phi}_{y(k+i-1)}$ and $\hat{\delta}^{\delta\phi}_{x(k+i-1)}$ as system states, the lateral errors between the vehicle and track centreline over the prediction horizon, $\hat{y}_{err(k+i)}$, can be formed as a system output together with $\hat{\phi}_{err(k+i)}$ and optimised within objective function (16).

E. Track Boundary and Tyre Slip Constraints

To prohibit the vehicle from crossing the track boundaries, constraints are imposed on the position of the vehicle. Since the position of the vehicle relative to the track has been linearised this is achieved straightforwardly by ensuring

$$\pm\hat{y}_{err(k+i)} \leq w_r/2 - w \quad (22)$$

for $i = 1 \dots N_p$, where w_r is the width of the track and w is the half-track-width of the vehicle. Furthermore, stabilising constraints on tyre lateral slip α_f and α_r are also included within the optimisation problem, limiting the tyres to operation within the positive slope region of the tyre force curves. Thus the lateral slip limit α_{bound} is set at, or just below, the point at which maximum lateral tyre force occurs.

$$\pm\hat{\alpha}_{j(k+i)} \leq \alpha_{bound}, \quad (23)$$

for $i = 1 \dots N_p$.

Equations (22) and (23) are incorporated into the optimisation problem through inequality (12).

IV. PATH OPTIMISATION SIMULATION RESULTS

To demonstrate the ability of the steering controller to control an oversteering vehicle, a number of simulations were performed. Figs. 5 and 6 show overlayed path and time-histories, respectively, for both a 90 deg and s-bend type manoeuvre. The s-bend manoeuvre was generated by coupling a right-hand 90 deg bend onto the initial left-hand 90 deg bend. The simulations were performed at a constant forward speed of 30 ms^{-1}. The simulation and control parameters used during the simulations are set out in Table II.

Fig. 5 shows how, at this demanding forward speed, the controller makes full use of the track width on both corner entry and exit. Furthermore, the rear axle side-slip time

TABLE II

SIMULATION AND CONTROL PARAMETERS USED DURING THE PATH OPTIMISATION SIMULATIONS.

Parameter	Symbol	Value
Discrete time step	T	0.02 s
Preview horizon	N_p	300
Maximise distance travelled weight	q	10
$\Delta\delta_{com}$ effort weight	R	1
Track/road width	w_r	10 m
Vehicle half track	w	0 m
Side-slip constraint	α_{bound}	0.09 rad

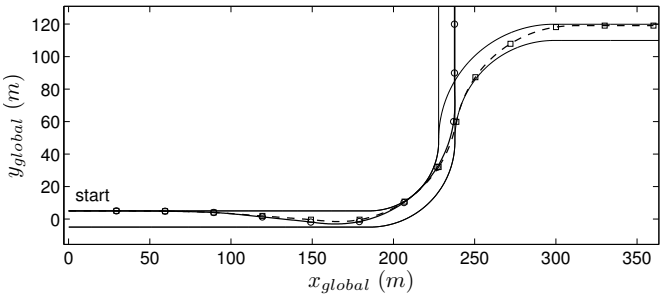

Fig. 5. Path optimised simulation results of an oversteering vehicle, for a 90 deg (solid line) and s-bend (dashed line) manoeuvre, with marked 1 second intervals.

histories demonstrate the controller operating the rear (limiting) axle on the imposed side-slip constraint corresponding to 99.8% peak lateral force, thus maximising the vehicle performance. In order to achieve this the controller applies counter-steering action during the approximately steady-state phases of the manoeuvre. The steering-wheel-angle (SWA) time histories also show how the oversteering motion is setup using the yaw dynamics to "flick" the vehicle one way then the other on corner entry. Further insight into the behaviour of the vehicle can be found by constructing a steady-state handling diagram for the nonlinear vehicle [13], as depicted in Fig. 7. Point **I** represents the operating point of the vehicle during approximately the 6-8 second phase of the path optimised simulation results. As can be seen, the vehicle operates at an equilibrium point just left of the rear slide point. Nevertheless this is well within the unstable region of its handling characteristics, demonstrating the steering controller is capable of controlling the vehicle model at the limit even during unstable operation. It is worth noting that because the vehicle is operating in an unstable region, application of these optimal controls to an equivalent nonlinear vehicle would likely result in the vehicle quickly deviating from the optimum path. In this case, a stabilising feedback controller would be needed to successfully complete the manoeuvre.

By overlaying the two simulated manoeuvres, provided the controller has sufficient preview, it is possible to compare the influence of a second corner on the vehicle trajectory through the first 90 deg bend. Fig. 5 shows that during the s-bend manoeuvre, the controller is able to use less track width on

corner entry and peel off from the first apex slightly earlier, taking advantage of the immediate transition into the second 90 deg bend. The different turn-in behaviour is somewhat a consequence of the constant speed restrictions imposed on the simulation, as a real driver would most likely use the full track width on entry in order to maximise the vehicle turn radius. Nonetheless, the results highlight the coupling between consecutive corners and how long preview horizons need to be used to compensate, to some extent, for the fact that a real racing driver is likely to have prior knowledge of the circuit layout.

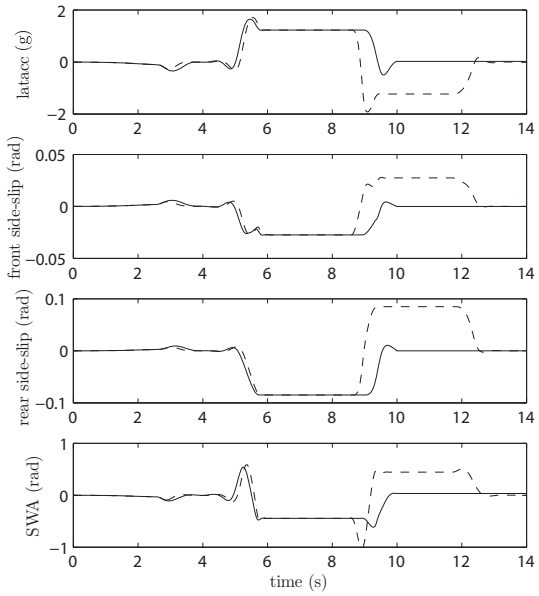

Fig. 6. Path optimised time histories, of a oversteering vehicle, for a 90 deg (solid line) and s-bend (dashed line) manoeuvre.

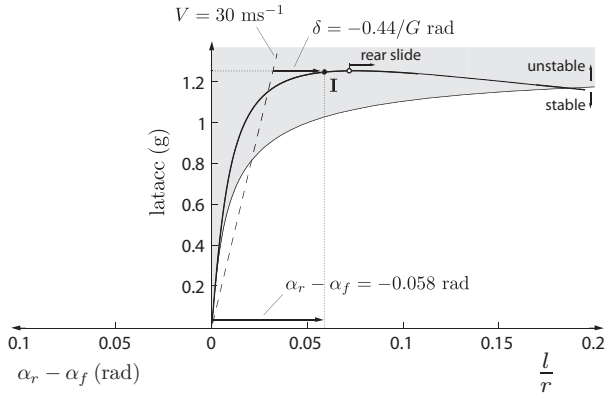

Fig. 7. Handling diagram resulting from normalised tyre characteristics. Steady-state equilibrium point **I**, represents the operating point of the vehicle during the 6-8 second phase of the path optimised simulations.

V. CONCLUSIONS

The work described details a steering controller capable of optimising the path of a vehicle, at constant forward speed, in order to minimise vehicle manoeuvre time. The problem has been formulated in a computational efficient and robust way by using linear time varying model predictive control theory and by linearising the positioning of the vehicle relative to the track. In particular, the novel approach used to linearise the vehicle position, describing the vehicle and reference path intrinsically and making use of the previous optimisation results, has enabled the optimisation problem to be formed as a convex Quadratic Programming problem. The use of long control and preview horizons has motivated significant computational gains to be achieved by adopting a banded structured MPC scheme, as opposed to the more widely documented densely structured approach.

Simulations have demonstrated the model can successfully control an oversteering nonlinear vehicle at its (unstable) lateral limit, with the same levels of limit-axle tyre saturation previously documented when controlling a stable understeering vehicle [8]. Operation of the vehicle at its handling limits has allowed the total vehicle distance travelled during the simulated manoeuvres to be minimised within the track boundary constraints. Future work includes the extension of the minimum manoeuvre time algorithm to combined optimal path and speed profile generation while controlling a more complex vehicle model.

VI. ACKNOWLEDGMENTS

The authors gratefully acknowledge the financial contribution of the UK Engineering and Physical Science Research Council and Lotus Renault GP.

REFERENCES

[1] D. Brayshaw and M. Harrison, "A quasi steady state approach to race car lap simulation in order to understand the effect of racing line and centre of gravity location," *Proceedings of IMechE - Part D: Journal of Automobile Engineering*, vol. 219, pp. 725–739, 2005.

[2] J. Blasco-Figueroa, "Minimum time manoeuvre based in the gg-speed envelope," Master's thesis, School of Engineering, Cranfield University, 2000.

[3] M. Thommyppillai, S. Evangelou, and R. S. Sharp, "Car driving at the limit by adaptive linear optimal preview control," *Vehicle System Dynamics*, vol. 47(12), pp. 1535–1550, 2009.

[4] ——, "Advances in the development of a virtual car driver," *Multibody System Dynamics*, vol. 22, pp. 245–267, 2009.

[5] D. Casanova, "On minimum time vehicle manoeuvring: The theoretical optimal lap," Ph.D. dissertation, School of Mechanical Engineering, Cranfield University, 2000.

[6] D. P. Kelly, "Lap time simulation with transient vehicle and tyre dynamics," Ph.D. dissertation, Cranfield University School of Engineering, 2008.

[7] M. Gerdts, S. Karrenberg, B. Muller-BeBler, and G. Stock, "Generating locally optimal trajectories for an automatically driven car," *Optimization and Engineering*, 2008.

[8] J. P. Timings and D. J. Cole, "Minimum manoeuvre time of a non-linear vehicle at constant forward speed using convex optimisation," in *Proceedings of The 10th International Symposium on Advanced Vehicle Control, Loughborough, UK*, 2010.

[9] S. D. Keen, "Modeling driver steering behaviour using multiple-model predictive control," Ph.D. dissertation, Department of Engineering, University of Cambridge, 2008.

[10] A. Odhams, "Identification of driver steering and speed control," Ph.D. dissertation, Department of Engineering, University of Cambridge, 2006.

[11] J. Maciejowski, *Predictive Control with Constraints*. Prentice-Hall: London, 2002.

[12] C. V. Rao, S. J. Wright, and J. B. Rawlings, "Application of interior-point methods to model predictive control," *Journal of Optimization Theory and Applications*, vol. 99, pp. 723–757, 1998.

[13] H. Pacejka, *Tyre and Vehicle Dynamics*, 2nd, Ed. Butterworth-Heinemann, 2006.